

Robust Metallic Lithium Anode Protection by the Molecular-Layer-Deposition Technique

Yang Zhao, Lyudmila V. Goncharova, Qian Sun, Xia Li, Andrew Lushington, Biqiong Wang, Ruying Li, Fang Dai, Mei Cai,* and Xueliang Sun*

The Li metal anode is considered as a promising alternative candidate for next-generation Li metal batteries with high specific capacity, low potential, and light weight. However, the crucial problem for the Li metal anode is one of the biggest challenges. Mossy or dendritic growth of Li occurs in the repetitive Li stripping/plating process with an unstable solid electrolyte interphase (SEI) layer of nonuniform ionic flux, which can not only lead to low Coulombic efficiency, but can also create the risk of a short-circuit, resulting in possible burning or explosion. Here, an advanced molecular-layer-deposition (MLD) Alucone protective layer is first demonstrated for Li metal anodes. By protecting Li foil with a controllable Alucone layer, the dendrites and mossy Li formation are effectively suppressed and the lifetime is significantly improved in different electrolytes (carbonate-based and ether-based). Furthermore, the detailed surface changes are studied by the advanced characterization technique of Rutherford backscattering spectrometry. The novel design of the MLD-protected Li metal anode may bring in new opportunities to the realization of the next-generation high-energy-density Li metal batteries.

1. Introduction

Recently, the depletion of fossil fuels and environment pollution has become a forefront issue and a serious hindrance to the development of a sustainable global economy^[1] Therefore, the exploration and usage of clean and sustainable energy as well as the development of systems and devices for energy storage and conversion is necessary.^[2] Rechargeable lithium-ion batteries (LIBs) have drawn great attention recently because of their high energy density, minimal self-discharge, and no memory effect, indicating potential application in portable electronics, electric vehicles, and renewable energy industries.^[3] Compared with commercial LIBs, Li-metal batteries (LMBs),

including Li-S batteries, Li-air batteries, and all-solid-state batteries, have been strongly considered as next-generation devices with high theoretical energy density (2600 Wh kg⁻¹ for Li-S and 11 680 Wh kg⁻¹ for Li-air).^[4] For LMBs, metallic Li is an ideal anode materials due to its high specific capacity (3860 mAh g⁻¹), low potential (-3.04 V vs the standard hydrogen electrode), and light weight (0.53 g cm⁻³) as well as the high energy density of 11 680 Wh kg⁻¹, which is nearly equivalent to gasoline.^[5] However, a number of issues, such as dendrite growth and volume change, plague the successful application of lithium metal for practical devices. The constant stripping/plating process of Li in each cycle eventually leads to uneven surface morphology and further the mossy or dendritic Li growth with poor Coulombic efficiency (CE) as

active lithium is lost to side reactions (Figure 1).^[6,7] In this case, it can cause two critical problems for Li metal, one is safety hazards because of potential internal short circuits and another is short cycle life. Even more serious, safety issues like smoke or fire and other hazards will be caused by the dramatic failure of the batteries.^[7]

One of the key points for metallic Li anode is the formation of a solid electrolyte interphase (SEI) layer, which is formed during the initial charging/discharging processes as a result of reaction between Li metal and different components in the electrolyte. Although the SEI formation will intrinsically consume both Li anode and electrolyte, leading to lower the CE, it can effectively prevent further contact and reactions between the Li anode and the electrolyte, making the Li anode stable in the electrolyte after a few initial cycles. It is considered that the unstable SEI layer is much easier to cause dendrite growth, in which the collapse of the SEI film can aggravate local dendrite growth and undesired electrolyte decomposition due to non-homogeneous local current buildup.

In the past several decades, researchers have focused on developing various approaches to achieve a stable SEI layer for long life Li metal anode. These strategies can be generally divided into two parts: in situ SEI formation and ex situ artificial SEI film.^[8] On one hand, the in situ formation of stable SEI film is developed by adjusting the electrolyte composition and additives.^[9,10] However, it is considered that mechanical strength of these in situ formed protective films is not high

Y. Zhao, Dr. Q. Sun, Dr. X. Li, A. Lushington, B. Wang, R. Li, Prof. X. Sun
Department of Mechanical and Materials Engineering
University of Western Ontario
London, Ontario N6A 5B9, Canada
E-mail: xsun@eng.uwo.ca

Prof. L. V. Goncharova
Department of Physics and Astronomy
University of Western Ontario
London, Ontario N6A 3K7, Canada

Dr. F. Dai, Dr. M. Cai
General Motors R&D Center
Warren, MI 48090-9055, USA
E-mail: mei.cai@gm.com

DOI: 10.1002/smt.201700417

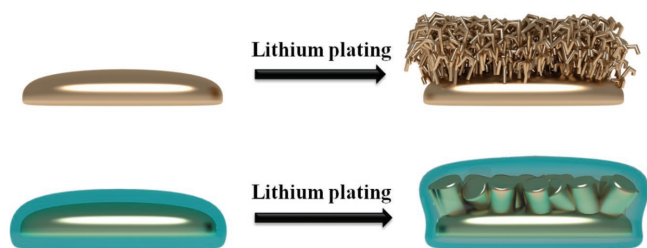


Figure 1. Schematic diagrams of lithium stripping/plating on bare Li foil and Li foil with MLD coating.

enough to withstand the large volume change during Li plating/stripping process.^[11] On the other hand, an effective approach is to develop novel coating layers on metallic Li in the form of an ex situ SEI film to reduce or prevent dendrite growth. Different types of coating layers have been applied on the surface of Li metal for dendrite prevention, including organic protective layers,^[12] inorganic protective layers,^[13] and organic–inorganic composite protective layer (CPL).^[14,15] For example, a Li-ion conductive inorganic/organic CPL has been developed as a coating on Li metal anode and has effectively suppressed dendrite growth and electrolyte decomposition, even under high current density.^[15]

However, challenges still remain for lithium protection and dendrite prevention, in which the controllable and uniform coating under low temperature (lower than the melting point of Li: 180.5 °C) is an issue for applying common method for thin film, e.g., chemical vapor deposition or any wet chemical method. Atomic layer deposition (ALD) can be an ideal technique which can achieve excellent coverage and conformal deposition under relatively low temperatures with precise control over coating thickness at the nanoscale level due to its self-limiting nature.^[16] Recently, two different groups have demonstrated ultrathin ALD Al₂O₃ coating film as a protective layer for metallic lithium.^[17] In their results, the ALD Al₂O₃-protected Li can prevent Li metal corrosion in electrolyte and reduce the dendrite growth as well, which further enhances electrochemical performance with elevated capacity and longer lifetimes. Very recently, our group also successfully demonstrated the protection of Na metal anode using ALD Al₂O₃, yielding extended life time and reduced growth of parasitic sodium dendrites.^[18] Molecular layer deposition (MLD), as an analogy of ALD, can be employed to produce pure polymeric thin films or inorganic–organic hybrid thin films, which can hold many advantages such, as lower growth temperatures, tunable thermal stability, and improved mechanical properties.^[19,20] Furthermore, the toughness and flexibility of polymeric metal thin films by MLD are strengthened with the introduction of C–C and C–O bonds in this system, which is expected to accommodate its huge volume expansion and dendrite growth of Li metal anode.^[21]

Here, we first demonstrate ultrathin MLD coating as a protective layer for metallic Li anode for improved lifetime and stability of Li metal anode. Compared with bare Li foil, MLD coating layer can stabilize the SEI film and further change the surface morphology of lithium growth. Meanwhile, the MLD coating layer can greatly improve the stability in both ether-based (used in Li–S batteries) and carbonate-based (used in Li-ion batteries) electrolyte, which is more promising compared

to ALD Al₂O₃ coating. Another interesting phenomenon is that the optimized thickness of MLD coating layer should be adjusted depending on the electrolytes used. Moreover, we also discuss the detailed surface change by advanced characterization techniques of Rutherford backscattering spectrometry (RBS). To the best of our knowledge, a powerful tool of RBS measurement is demonstrated for the first time in the field of Li metal anode, which gives the guidance to the researchers working in this area.

2. Results and Discussion

The Alucone (Al-EG) films were directly deposited on Li metal anode using trimethylaluminum (TMA) and ethylene glycol (EG) as precursors at 120 °C using a glovebox-integrated ALD tool. The growth rate of Alucone was evaluated by placing a silicon wafer in the deposition chamber at the same time as lithium foil. Alucone growth rate was determined by X-ray reflectometry to be ≈0.5 nm per cycle (Figure S1, Supporting Information). The influence of Alucone thickness is investigated in detail with 5, 10, 25, and 50 MLD cycles with a thickness of 2.5, 5, 10, and 25 nm, respectively (named as Li@5Alucone, Li@10Alucone, Li@25Alucone, and Li@50Alucone). X-ray photoelectron spectroscopy (XPS) is used to investigate the surface of Li foil after Alucone deposition, which is shown in Figure S2 (Supporting Information). Peaks at 70.15, 281.55, and 527.95 eV can be attributed to Al, C, and O, respectively. It can be demonstrated that the Alucone coating containing Al and EG has been successfully deposited on the Li foil. RBS was carried out on Al₂O₃-coated and Alucone-coated Li anodes before and after cycling. Figure S3 (Supporting Information) shows that as-deposited Al₂O₃ film forms a continuous layer ≈14 nm thick (assuming $\rho_{\text{Al}_2\text{O}_3} = 2.7 \text{ g cm}^{-3}$). Li surface peak is not observed; the best-fit model (Figure S3b, Supporting Information) assumes formation of the interfacial layer between Al₂O₃ and Li metal or Li surface roughness. Alucone film thickness (Figure S3d, Supporting Information) is also continuous and slightly thicker for the same number of MLD deposition cycles. The amount of O and C in the Alucone film is consistent with Al_n(CO)_m stoichiometry, with $n \approx m = 1$.

The galvanostatic cycling performance of Li with MLD Alucone coating layers and bare Li foil was studied in ether-based electrolyte, commonly employed in Li–S batteries (1 M LiTFSI in dioxolane (DOL): dimethoxyethane (DME) of 1:1 volume ratio with 1 wt% LiNO₃). Figure 2a shows the cycling stability of Li@10Alucone and bare Li foil at a current density of 3 mA cm⁻². For bare Li foil, the initial Li stripping/plating overpotential is ≈50 mV (vs Li⁺/Li) and rapidly increases to over 120 mV (vs Li⁺/Li) after 50 cycles. Following this, the overpotential of bare Li remains at 80 mV (vs Li⁺/Li) for up to 100 cycles. Protected Li, with 10 cycles of Alucone, shows a minor initial overpotential of about 100 mV (vs Li⁺/Li), which can be attributed to the formation of an ionically conductive SEI film between Alucone and Li. The overpotential of Li@10Alucone decreases after the first few cycles to 40 mV (vs Li⁺/Li) and maintains this overpotential over 100 cycles (50 mV vs Li⁺/Li). Figure 2b,c shows the detailed voltage profiles of Li@10Alucone and bare Li foil in the first cycle and after

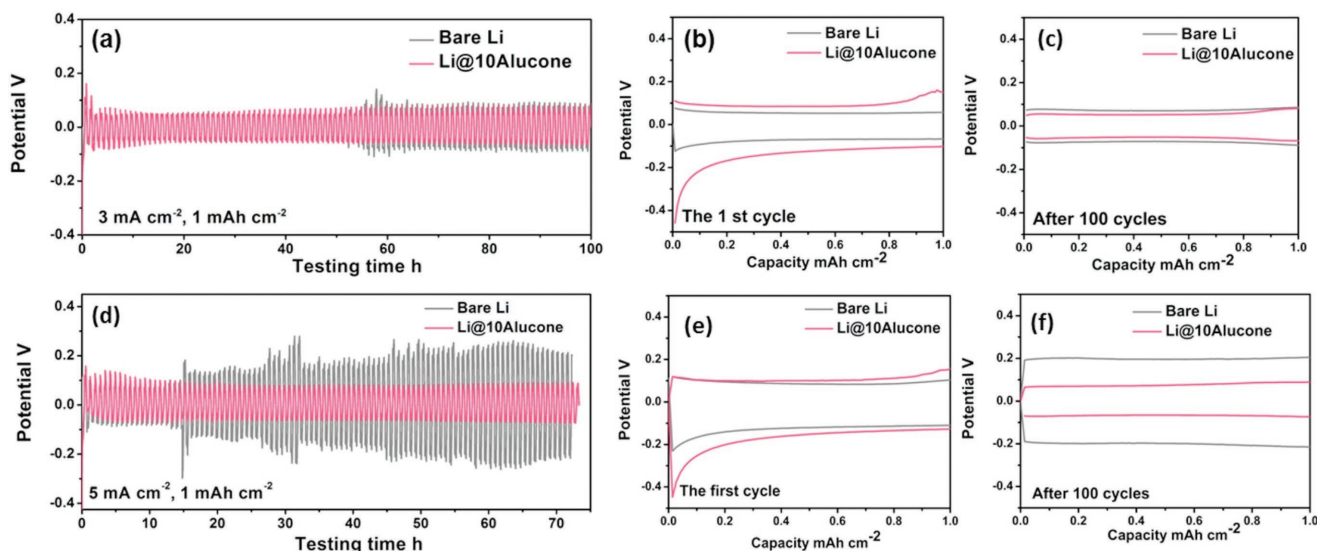


Figure 2. a) Comparison of the cycling stability of the Li@10Alucone cycles and the bare Li foil at a current density of 3 mA cm^{-2} in DOL/DME electrolyte; b,c) voltage profiles of Li@10Alucone cycles and bare Li foil in the first cycles (b) and after 100 cycles (c) at a current density of 3 mA cm^{-2} . d) Comparison of the cycling stability of the Li@10Alucone cycles and the bare Li foil at a current density of 5 mA cm^{-2} in DOL/DME electrolyte; e,f) voltage profiles of Li@10Alucone cycles and bare Li foil in the first cycles (e) and after 100 cycles (f) at a current density of 5 mA cm^{-2} . The amount of Li cycled was 1 mAh cm^{-2} .

100 cycles. Increasing the current density to 5 mA cm^{-2} , the initial Li stripping/plating overpotential for bare Li increases to 80 mV (vs Li/Li⁺). After 20 cycles, there is a sudden rise of overpotential to 160 mV (vs Li/Li⁺) with following fluctuations in overpotential voltage. Meanwhile, an obvious drop of voltage can be observed for the bare Li foil in around 43 cycles, which could be explained as a soft short-circuit with Li dendrite penetration. However, with 10 cycles of Alucone, the protected Li foil indicates a similar initial overpotential of 100 mV (vs Li/Li⁺) under the current density of 5 mA cm^{-2} . It also can be ascribed to the activated process for Li transportation. The protected Li is extremely stable over 100 cycles with an overpotential of 70 mV (vs Li/Li⁺), which is much lower than that of the bare Li (over 200 mV after 100 cycles). From the voltage profiles of Li@10Alucone at the current density of 5 mA cm^{-2} , a flat voltage plateau at both the charging and discharging states can be retained throughout the whole cycle with minimal increase in hysteresis (Figure 2e,f). It also should be noticed that the differences in the initial few cycles in the plating/stripping curves are attributed to the lithiation of Alucone and the stable SEI layer formation. To further explain the performances, electrochemical impedance spectroscopy was performed at the point of before cycling and after 50 cycles, as shown in Figure S7a–c (Supporting Information) and impedance parameters calculated by equivalent circuits for different samples are shown in Table S1 (Supporting Information). Figure S7a (Supporting Information) indicates the initial spectra with a slight increase in the impedance for the Li@10Alucone compared with bare Li foil before cycling. After 20 cycles of plating/stripping process (Figure S7b, Supporting Information), the R_{SEI} of both bare Li and Li@10Alucone decreases, in which the resistance of Li@10Alucone is lower than bare Li. Furthermore, resistance of bare Li maintains its resistance value over 50 cycles while Li@10Alucone further decreases (Figure S7c, Supporting

Information), demonstrating formation of a stable SEI layer with Alucone protection.

Furthermore, the protected Li foil with 10 cycles of Alucone coating shows superior stripping/plating performances with superlong lifetime, shows the long life cycling performances of Li@10Alucone at the current density of 3 mA cm^{-2} , in which the protected Li can work for more than 500 cycles (500 h) without any short circuit occurring. From the voltage profiles (Figure S4b, Supporting Information), the curves from the first cycle, 100 cycles, 300 cycles, and 500 cycles show a flat plateau at 50 mV (vs Li/Li⁺), indicating an extraordinary stable performance with superlong lifetime. Even at a high current density of 5 mA cm^{-2} (Figure S4c, Supporting Information), there is also no voltage fluctuation up to 500 cycles with flat plateaus occurring at 60 mV (vs Li/Li⁺).

In order to understand the influence of MLD Alucone coating on Li dendrite growth, morphology of lithium metal was imaged before and after cycling using scanning electron microscopy (SEM). SEM images of bare Li foil are shown in Figure 3a,b with a flat surface. After 10 cycles of MLD Alucone coating (Figure 3c,d), there is no obvious difference of the quite smooth surface due to the ultrathin thickness of coating layers ($\approx 5 \text{ nm}$). After 30 cycles of Li plating/stripping process at a current density of 3 mA cm^{-2} , unordered Li dendrite growth can be observed on the bare Li foil (Figure 3e,f) with protrusions of over $10 \mu\text{m}$ occurring. This growth can be attributed to the broken and repeatedly repaired SEI layer during cycling, resulting in serious growth of sharp Li dendrite. This type of Li dendrite growth can facily detach from the underlying foil, resulting in the formation of dead Li in subsequent plating and stripping, and will consume effective Li and lower the Coulombic efficiency. Furthermore, the sharp and long dendrite can penetrate the separator, causing a short circuit and detrimental safety issues. When increasing the current density to 5 mA cm^{-2} , after

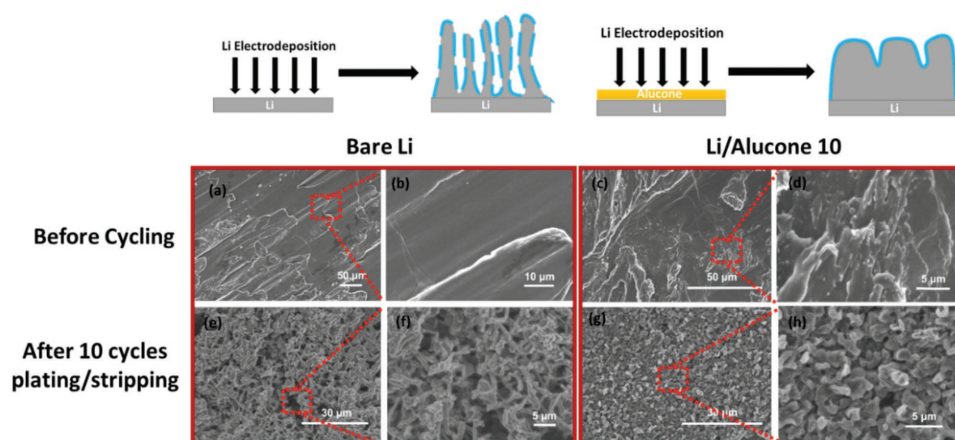


Figure 3. a–d) Top-view SEM images of bare Li (a,b) and Li@10Alucone cycles (c,d); e–h) top-view SEM images of bare Li (e,f) and Li@10Alucone (g,h) after 30 cycles of stripping/plating in DOL/DME electrolyte at a current density of 3 mA cm^{-2} . The amount of Li cycled was 1 mAh cm^{-2} .

30 cycles of plating/stripping similar Li dendrite growth can be observed (Figure S8, Supporting Information). Promisingly, the morphology of the cycled Li with Alucone coating is drastically different. Figure 3g,h shows the SEM images of Li@10Alucone after 30 cycles of stripping/plating under a current density of 3 mA cm^{-2} . With the assistance of MLD, the Li dendrites exhibit a nodule-like structure with round-shaped edges and present very dense structure on the surface of Li anode.^[10] Even at an elevated current density of 5 mA cm^{-2} , uniform growth of the reduced Li dendrites can be observed. The larger dimension of nodule-like dendrites can effectively limit their penetration through the separator. Furthermore, this diminished dendrite growth can effectively reduce the high surface area caused by mossy dendrites growth on the bare Li foil (Figure 3g,h), which can decrease the contact area between electrolyte and Li. Meanwhile, this kind of structure can be well maintained during the cycling, resulting in better performance and longer lifetime. It can be considered that with the protection of Alucone, the SEI film is expected to be stabilized with good mechanical strength and ionic conductivity.

The thickness effect of MLD Alucone coating has also been investigated with MLD cycle numbers of 5, 25, and 50 in Figure S5, Supporting Information. Figure S5a,e shows the Li plating/stripping performances of protected Li with 5 cycles of Alucone coating. The cycling performances of Li@5Alucone are more stable than the bare Li foil without any fluctuation of voltage. However, the overpotentials of Li@5Alucone after 100 cycles at the current density of 3 and 5 mA cm^{-2} are 70 and 80 mV (vs Li/Li⁺), respectively, which is a little higher than 10 cycle Alucone-coated Li foil, demonstrating an increase in hysteresis with less Alucone coatings. When increasing the Alucone coating to 25 cycles (Figure S5b,f, Supporting Information), the cycling stability during plating/stripping is still very promising compared to bare Li. The overpotentials after 100 cycles at a current density of 3 and 5 mA cm^{-2} are 50 and 70 mV, respectively, which are similar with the results of 10 cycles of Alucone coating. However, when applying a thicker coating of 50 cycles, although stable plating/stripping performance is achieved, the overpotential is much higher than the protected Li with 10 and 25 cycles of Alucone (Figure S6, Supporting Information). The

results demonstrate that the optimizing of Alucone thickness is an important factor for the electrochemical performances of protected Li foil during plating/stripping process, in which too thin (five cycles of Alucone) or too thick (50 cycles of Alucone) coatings can achieve stable cycling performances but higher resistance. Meanwhile, the morphologies of electrodes with 5 and 25 cycles of Alucone are also investigated, as shown in Figure S9 and Figure S10 (Supporting Information). With thinner coating (five cycles), it has been partial improved for dendrite growth, in which sharp and long Li dendrite still can be seen on the surface. When increasing the number of Alucone cycles to 25, the similar structure with dense and shorter rod-like Li is formed which is consistent with the electrochemical performances with different cycles discussed above. So, the optimal thickness of MLD Alucone protective coating layer is 10–25 cycles.

It is well known that dendrite growth in carbonate-based electrolyte is more serious than in ether-based electrolyte. We also applied Alucone-coated Li in carbonate-based electrolyte (1 M LiPF₆ in ethylene carbonate (EC): DEC: EMC of 1:1:1 volume ratio) to study the Li plating/stripping performances. For pure Li foil, obvious voltage fluctuations can be observed after about 300 h of plating/stripping, with a rapid increase in overpotential occurring, indicating the ceaseless increase of resistance in the system and short circuit happening during this time (Figure 4a). It is very promising that with the protective coating layers of Alucone, the polarization curve is more stable than the bare Li foil (Figure 4a). In the above discussion, Li foil with 10 cycles of Alucone coating in ether-based electrolyte shows the best plating/stripping performances. Interestingly, in the carbonate electrolyte, 10 cycles of Alucone coating are not enough to form a stable SEI film and demonstrate a slow rise in voltage. From Figure 4a, it can be found that when increasing thickness to 50 cycles of Alucone, the most stable plating/stripping performances can be achieved. The voltage profiles in Figure 4b,c indicate a constant potential with almost no change in Li@50Alucone after one cycle and 140 cycles of plating/stripping. Thus, MLD Alucone coating can be an excellent candidate for the protection of Li metal anode for both ether-based and carbonate-based electrolyte with long cycle life and superior stability. Meanwhile, our study also demonstrates

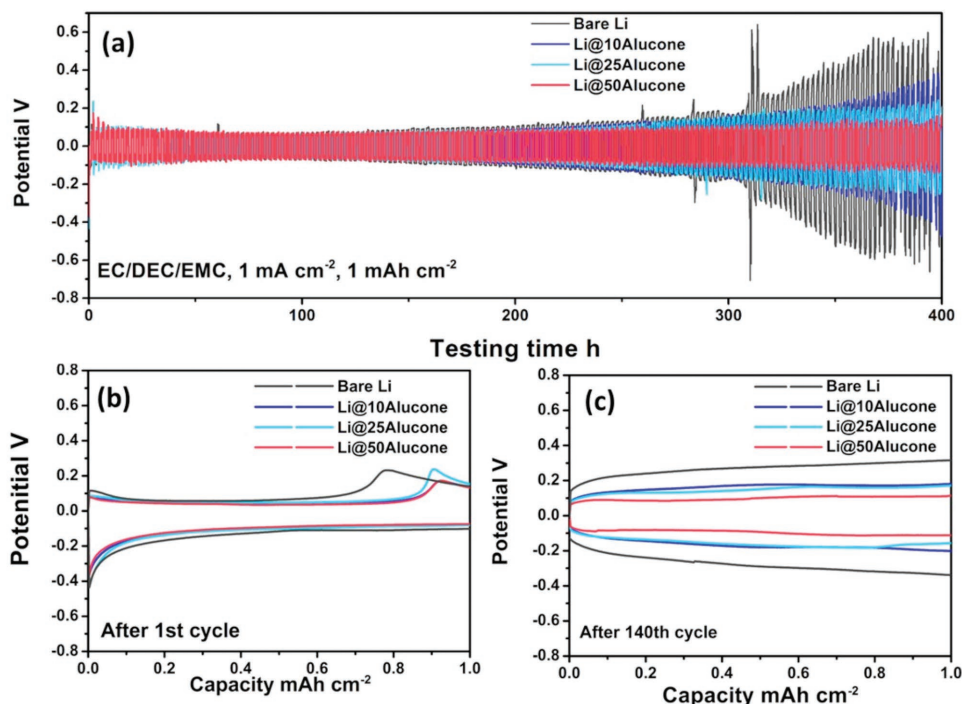


Figure 4. a) Comparison of the cycling stability of the bare Li foil, Li@10Alucone, Li@25Alucone, and Li@50Alucone at a current density of 1 mA cm⁻² in EC/DEC/EMC electrolyte; b,c) voltage profiles of Li foil, Li@10Alucone, Li@25Alucone, and Li@50Alucone in the first cycles (b) and after 140 cycles (c) at a current density of 1 mA cm⁻².

that the thickness of the Alucone coating should be optimized based on the electrolyte system that needs to be employed. It can be considered that a thinner coating layer is needed for ether-based electrolyte (DOL/DME), which can easily form a stable SEI layer with Alucone coating (10 cycles). For the carbonate-based electrolyte (EC/DEC/EMC), a thicker coating (50 cycles) is required to form a stable SEI.

ALD Al₂O₃ has also been investigated as protective coating for Li metal anode. The same glove-box contact ALD system was applied to deposit Al₂O₃, using TMA and water as precursor at 120 °C, in which the growth rate of Al₂O₃ under this condition is about 0.1 nm per cycle. First, the thickness of ALD Al₂O₃ has also been optimized based on the Li plating/stripping performances in two types of electrolyte system. Figure S11 (Supporting Information) shows the cycling stability

of Li foil with different cycles of ALD Al₂O₃ coating, including 10, 25, and 50 cycles, in which the protected Li metal anode with 25 cycles of Al₂O₃ coating has the best performance and lowest overpotential in ether-based electrolyte (DOL/DME). In the carbonate-based electrolyte, similar results are present in Figure S12 (Supporting Information), in which the optimized thickness of Al₂O₃ coating is still 25 cycles. Then, **Figure 5** compares the plating/stripping performance of Al₂O₃ and Alucone coated Li. When testing in ether-based electrolyte (DOL/DME), both Al₂O₃ and Alucone show more stable polarization curves compared with bare Li foil. More obvious difference can be observed from Figure 5a in the carbonate-based electrolyte. As discussed above, the bare Li foil only can be stabilized for 300 h with the unexpected short circuit. With 25 cycles of Al₂O₃ coating, although there is no short circuit over 190 cycles, the

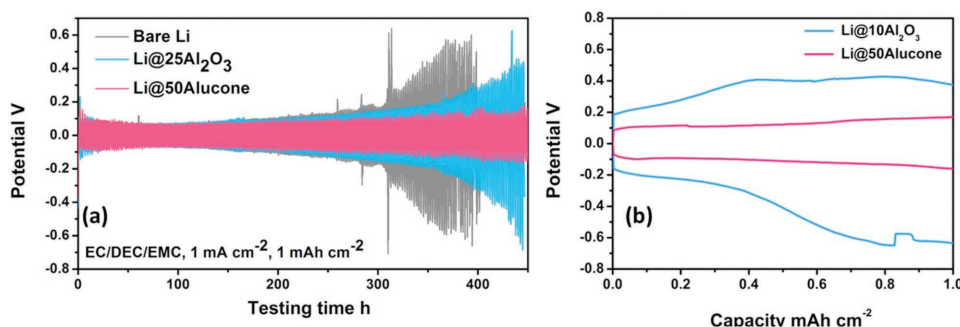


Figure 5. a) Comparison of cycling performance between bare Li, Li@25Al₂O₃, and Li@50Alucone in EC/DEC/EMC electrolyte at the current density of 1 mA cm⁻²; b) voltage profiles of Li@50Alucone and Li@25Al₂O₃ after 190 cycles at the current density of 1 mA cm⁻² in EC/DEC/EMC electrolyte.

voltage is continuously raised up after 300 h, declaring the increasing resistance and instability of SEI film in long time cycling. Promisingly, Li@50Alucone indicates superstable plating/stripping performances over 480 h (equal to 190 cycles). From the voltage profiles in Figure 5b, the overpotential of Li@25Al₂O₃ is over 420 mV after 190 cycles; however, it is only 160 mV for Li@50Alucone. From the electrochemical plating/stripping performances, it indicates that optimized Alucone coating is more effective to form the stable SEI layer achieving long life Li metal anode compared with Al₂O₃ in both carbonate-based and ether-based electrolytes. It is believed that Alucone coating is highly stable against liquid electrolyte and acts as a passivating agent to assist Li metal anode to form a stable SEI layer. Meanwhile, Alucone coating is mechanically flexible and allows for repeated Li plating/stripping on the surface of Li foil. Furthermore, it is also considered that after lithiation, Alucone coating has high Li⁺ conductivity with the porous structure for Li ions transport.^[19,22]

In order to elucidate compositional changes following the plating/stripping cycling experiments, RBS measurements were performed for all samples. **Figure 6a** shows RBS spectra for bare Li, as well as Li coated with 25 cycles of ALD Al₂O₃ and 50 cycles of MLD Alucone films all after 10 cycles in carbonate-based electrolyte (1 M LiPF₆ in EC/DEC/EMC). While bare Li shows significant penetration of P and F from electrolyte into subsurface layer, as well as oxidation, Al₂O₃- and Alucone-films act as good protective barriers, with small concentrations of P, F, and C localized in the first 70–100 nm from the surface. Notably, Li@50 Alucone film mostly remains as a continuous film as evident from relatively sharp Al, O, and C peaks, and very little changes in composition compared to as-deposited Alucone film (Figure S3d, Supporting Information). In this case, it can be seen that both ALD Al₂O₃ and MLD Alucone coating can effectively reduce the reactions and penetration of electrolyte with Li metal. Meanwhile, the ALD Al₂O₃ protective layer will be fractured and MLD Alucone film can remain the better structure after 10 cycles of electrochemical plating/stripping (Figure 6e), indicating that Alucone is the stronger and

more robust film during cycling. Effects of cycling in DOL/DME electrolyte on elemental depth profiles are illustrated in Figure S13 (Supporting Information). More substantial diffusion processes are evident after plating/stripping in more aggressive DOL/DME electrolyte. Al peak is not observed for Li@25Al₂O₃ sample, indicating either removal of all Al or significant growth of Li on top Al₂O₃ layer. Al peak is still detectable for Li@50Alucone sample; however, Al depth profile goes deeper, consistent with significant morphological changes detected in SEM and Li diffusion.

For investigating the full-cell performance, the Li–S coin cells were assembled with C/S composites as cathode electrode in the ether-based electrolyte. The long-term cycling performance of these cells is shown in Figure S14 (Supporting Information). For the bare Li anode, an obvious capacity fade of C/S cathode can be observed due to the self-propagating reaction since the dissolved polysulfides enable to react with Li metal and finally form insulated Li₂S deposited on Li foil. After 100 cycles, the capacity and CE of the cell remain only 486 mAh g⁻¹ and 84%, respectively. Very promising, with MLD Alucone protective coating, the cell can be stabilized after initial 10 cycles and both the reversible capacities and CE have been significantly improved after 100 cycles (711 mAh cm⁻² and 95%). It can be expected that the MLD Alucone coating can increase the long lifetime of the cell and improve the utilization of the sulfur by prevention of the corrosion and reaction between Li and polysulfide.

In conclusion, we first demonstrate the use of an MLD protective coating on Li metal anode for long life Li metal batteries. By protected Li foil with ultrathin Alucone layer, the sharp and long dendrites Li formation have been effectively suppressed and lifetime has been significantly improved. Meanwhile, we reveal a comprehensive study of Alucone coating in both ether-based and carbonate-based electrolyte, both resulting in significant improvement on the plating/stripping performance of lithium metal. Remarkably, we also find that the thickness of Alucone coating should be optimized based on the electrolyte employed. Ether-based electrolytes (DOL/DME) demonstrate

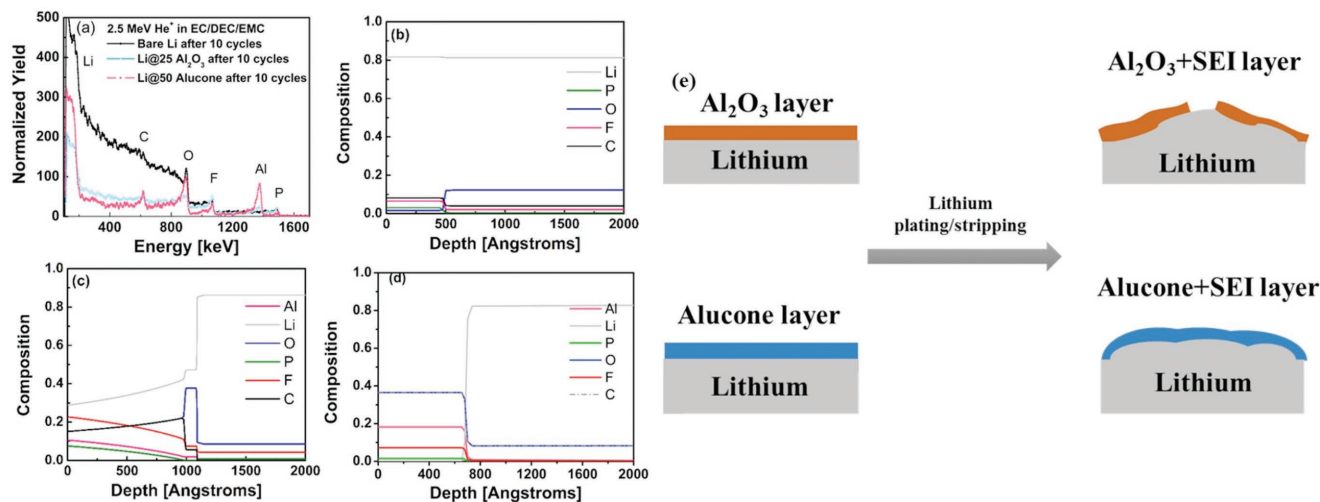


Figure 6. a) Comparison of RBS spectra for bare Li, Li@25Al₂O₃, and Li@50Alucone after 10 cycles in EC/DEC/EMC electrolyte; b–d) calculated depth profiles, and e) schematic diagrams illustrating morphological changes in the films.

the best performance when using 10 cycles of Alucone coating and enables the formation of a stable SEI film with restrained dendrite growth. However, for carbonate-based electrolytes (EC/DEC/EMC), a thicker coating of 25 cycles of Alucone is needed to achieve stable performance. Furthermore, a comparison between ALD Al_2O_3 and MLD Alucone has also been presented in detail for both electrolyte systems. Based on the plating/stripping performances, Alucone is more promising with longer lifetime, stable polarization curve, and lower internal resistance compared with Al_2O_3 , especially in carbonate-based electrolyte. It is believed that our design of MLD Alucone-coated metal Li anode open up new opportunities to the realization of the next-generation high-energy-density Li metal batteries.

3. Experimental Section

Electrode Preparation: Li foil was purchased from China Energy Lithium Co. LTD with further polishing before using, which was stored in the argon-filled glovebox. MLD of Alucone coatings was conducted in a Gemstar-8 ALD system (Arradance, USA) directly connected with argon-filled glovebox. Alucone was directly deposited on the Li foil at 120 °C by alternatively introducing TMA and EG as precursors. The MLD process used as 0.01/40/0.01/70 s TMA pulse/purge/EG pulse/purge sequence with a growth rate of 0.5 nm per cycle. The different cycle numbers of 5, 10, 25, and 50 MLD Alucone coating on Li foil were named as Li@5Alucone, Li@10Alucone, Li@25Alucone, and Li@50Alucone, respectively.

For comparison, ALD Al_2O_3 was performed using TMA and H_2O as precursors at 120 °C. The ALD process used as 0.01/30/0.01/50 s TMA pulse/purge/ H_2O pulse/purge sequence with a growth rate of 0.1 nm per cycle. The different cycle number of 10, 25, and 50 ALD Al_2O_3 had been coated on the Li foil named as Li@10 Al_2O_3 , Li@25 Al_2O_3 , and Li@50 Al_2O_3 , respectively.

Electrochemical Measurements: The electrochemical analysis was performed in CR2032 coin-type cells. The coin cells were assembled in an ultrapure argon-filled glovebox by symmetrical Li/electrolyte-separator/Li system using polypropylene separator (Celgard 2400). The electrolyte used in this study was a 1 M LiTFSI salt in DOL:DME of 1:1 volume ratio with 1% lithium nitrate, which was used by the group for Li-S studies. The stripping/plating studies were carried out in an Arbin BT-2000 Battery Test System at room temperature. A constant current was applied to the electrodes during repeated stripping/plating, while the potential was recorded over time.

Another carbonate-based electrolyte was also used for comparison, which is 1 M LiPF₆ salt dissolved in EC: DEC: EMC of 1: 1: 1 volume ratio.

Lithium-sulfur batteries were tested via CR2032 cells using protected Li (Li@50Alucone) and C/S cathode with 1 M LiTFSI in DOL: DME 1:1. The carbon-sulfur (C-S) composite was synthesized by using commercial carbon black (KJ EC-600, US), mixed with sulfur powder (99.5%, Sigma-Aldrich), and dried at 80 °C for 12 h to remove moisture. The carbon-sulfur mixture was then transferred to a sealed steel reactor and was heated at 150 °C for 9 h and then 300 °C for 3 h. The obtained C-S composites maintained 70 wt% sulfur loading. The electrodes were prepared by slurry casting onto aluminum foil. The slurry mass ratio of active material, acetylene black, and polyvinylidene fluoride is 80:10:10. The as-prepared electrodes were finally dried at 80 °C over 12 h under vacuum. The areal loading of sulfur in cathode electrode is about 0.9–1.2 mg cm⁻². Charge-discharge characteristics were galvanostatically tested in the range of 1.0–3.0 V (vs Li/Li⁺) at room temperature using a Landlike Battery Test equipment.

Characterization: SEM images were taken using a Hitachi 3400N environmental SEM at an acceleration voltage of 5 kV. Due to the soft properties of Li metal, Swagelok type cells comprised of Li/electrolyte-separator/Li system were used to carry out the morphology testing after stripping/plating. The Swagelok cells were disassembled after 30 cycles

of stripping/plating process under the different current density. The Alucone-coated Li foil was transferred from the ALD glovebox directly to an Ar glovebox connected XPS (Kratos AXIS Ultra Spectrometer) system for XPS analysis. Rutherford backscattering spectrometry measurements were conducted using 1 and 2.5 MeV He⁺ beam (Western Tandemron Facility) at several locations on the surface to confirm the uniformity of the thicknesses and composition. All samples were transferred in Ar-filled glove bag with minimum exposure to air. A Sb-implanted amorphous Si sample with a known 4.82×10^{15} atoms cm⁻² Sb content was used for calibration.

Supporting Information

Supporting Information is available from the Wiley Online Library or from the author.

Acknowledgements

This research was supported by the Natural Science and Engineering Research Council of Canada (NSERC), the Canada Research Chair Program (CRC), the Canada Foundation for Innovation (CFI), and the University of Western Ontario (UWO).

Conflict of Interest

The authors declare no conflict of interest.

Keywords

atomic layer deposition, lithium protection, metallic lithium anode, molecular layer deposition, Rutherford backscattering spectrometry

Received: December 28, 2017

Revised: January 9, 2018

Published online: March 26, 2018

- [1] G. Wang, L. Zhang, J. Zhang, *Chem. Soc. Rev.* **2012**, *41*, 797.
- [2] Y. Wang, R. Chen, T. Chen, H. Lv, G. Zhu, L. Ma, C. Wang, Z. Jin, J. Liu, *Energy Storage Mater.* **2016**, *4*, 103.
- [3] a) W. Lv, Z. Li, Y. Deng, Q.-H. Yang, F. Kang, *Energy Storage Mater.* **2016**, *2*, 107; b) M. Yu, R. Li, M. Wu, G. Shi, *Energy Storage Mater.* **2015**, *1*, 51; c) Y. Zhao, X. Li, B. Yan, D. Xiong, D. Li, S. Lawes, X. Sun, *Adv. Energy Mater.* **2016**, *6*, 1502175; d) K. Zhao, L. Zhang, R. Xia, Y. Dong, W. Xu, C. Niu, L. He, M. Yan, L. Qu, L. Mai, *Small* **2016**, *12*, 588; e) K. Zhao, M. Wen, Y. Dong, L. Zhang, M. Yan, W. Xu, C. Niu, L. Zhou, Q. Wei, W. Ren, X. Wang, L. Mai, *Adv. Energy Mater.* **2017**, *7*, 1601582.
- [4] J. Wang, Y. Li, X. Sun, *Nano Energy* **2013**, *2*, 443.
- [5] a) D. Lin, Y. Liu, Z. Liang, H. W. Lee, J. Sun, H. Wang, K. Yan, J. Xie, Y. Cui, *Nat. Nanotechnol.* **2016**, *11*, 626; b) Y. Liu, D. Lin, Z. Liang, J. Zhao, K. Yan, Y. Cui, *Nat. Commun.* **2016**, *7*, 10992.
- [6] a) J. T. Vaughey, G. Liu, J.-G. Zhang, *MRS Bull.* **2014**, *39*, 429; b) D. Lin, Y. Liu, Y. Cui, *Nat. Nanotechnol.* **2017**, *12*, 194.
- [7] W. Xu, J. Wang, F. Ding, X. Chen, E. Nasybulin, Y. Zhang, J.-G. Zhang, *Energy Environ. Sci.* **2014**, *7*, 513.
- [8] a) R. Younesi, G. M. Veith, P. Johansson, K. Edström, T. Vegge, *Energy Environ. Sci.* **2015**, *8*, 1905; b) X.-B. Cheng, R. Zhang, C.-Z. Zhao, F. Wei, J.-G. Zhang, Q. Zhang, *Adv. Sci.* **2016**, *3*, 1500213; c) Z. Li, J. Huang, B. Yann Liaw, V. Metzler, J. Zhang, *J. Power Sources* **2014**, *254*, 168.

- [9] a) W. Li, H. Yao, K. Yan, G. Zheng, Z. Liang, Y. M. Chiang, Y. Cui, *Nat. Commun.* **2015**, *6*, 7436; b) J. Qian, W. Xu, P. Bhattacharya, M. Engelhard, W. A. Henderson, Y. Zhang, J.-G. Zhang, *Nano Energy* **2015**, *15*, 135.
- [10] J. Qian, W. A. Henderson, W. Xu, P. Bhattacharya, M. Engelhard, O. Borodin, J. G. Zhang, *Nat. Commun.* **2015**, *6*, 6362.
- [11] Z. Liang, G. Zheng, C. Liu, N. Liu, W. Li, K. Yan, H. Yao, P. C. Hsu, S. Chu, Y. Cui, *Nano Lett.* **2015**, *15*, 2910.
- [12] a) N. S. Choi, Y. M. Lee, W. Seol, J. A. Lee, J. K. Park, *Solid State Ionics* **2004**, *172*, 19; b) N.-S. Choi, Y. M. Lee, K. Y. Cho, D.-H. Ko, J.-K. Park, *Electrochem. Commun.* **2004**, *6*, 1238; c) G. Ma, Z. Wen, Q. Wang, C. Shen, J. Jin, X. Wu, *J. Mater. Chem. A* **2014**, *2*, 19355; d) C. B. Bucur, A. Lita, N. Osada, J. Muldoon, *Energy Environ. Sci.* **2016**, *9*, 112.
- [13] a) K. Yan, H. W. Lee, T. Gao, G. Zheng, H. Yao, H. Wang, Z. Lu, Y. Zhou, Z. Liang, Z. Liu, S. Chu, Y. Cui, *Nano Lett.* **2014**, *14*, 6016; b) G. Zheng, S. W. Lee, Z. Liang, H. W. Lee, K. Yan, H. Yao, H. Wang, W. Li, S. Chu, Y. Cui, *Nat. Nanotechnol.* **2014**, *9*, 618; c) H.-K. Jing, L.-L. Kong, S. Liu, G.-R. Li, X.-P. Gao, *J. Mater. Chem. A* **2015**, *3*, 12213; d) Y. J. Zhang, W. Wang, H. Tang, W. Q. Bai, X. Ge, X. L. Wang, C. D. Gu, J. P. Tu, *J. Power Sources* **2015**, *277*, 304.
- [14] a) D. J. Lee, H. Lee, J. Song, M.-H. Ryou, Y. M. Lee, H.-T. Kim, J.-K. Park, *Electrochem. Commun.* **2014**, *40*, 45; b) D. J. Lee, H. Lee, Y.-J. Kim, J.-K. Park, H.-T. Kim, *Adv. Mater.* **2016**, *28*, 857.
- [15] H. Lee, D. J. Lee, Y.-J. Kim, J.-K. Park, H.-T. Kim, *J. Power Sources* **2015**, *284*, 103.
- [16] a) X. Meng, X. Q. Yang, X. Sun, *Adv. Mater.* **2012**, *24*, 3589; b) J. Liu, X. Sun, *Nanotechnology* **2015**, *26*, 024001; c) X. Li, J. Liu, M. N. Banis, A. Lushington, R. Li, M. Cai, X. Sun, *Energy Environ. Sci.* **2014**, *7*, 768.
- [17] a) C.-F. L. Alexander, C. Kozen, J. Alexander Pearse, A. Marshall Schroeder, X. Han, L. Hu, S.-B. Lee, G. W. Rubloff, M. Noked, *ACS Nano* **2015**, *9*, 5884; b) E. Kazyak, K. N. Wood, N. P. Dasgupta, *Chem. Mater.* **2015**, *27*, 6457.
- [18] Y. Zhao, L. V. Goncharova, A. Lushington, Q. Sun, H. Yadegari, B. Wang, W. Xiao, R. Li, X. Sun, *Adv. Mater.* **2017**, *29*, 1606663.
- [19] X. Li, A. Lushington, J. Liu, R. Li, X. Sun, *Chem. Commun.* **2014**, *50*, 9757.
- [20] X. Li, A. Lushington, Q. Sun, W. Xiao, J. Liu, B. Wang, Y. Ye, K. Nie, Y. Hu, Q. Xiao, R. Li, J. Guo, T. K. Sham, X. Sun, *Nano Lett.* **2016**, *16*, 3545.
- [21] Y. Zhao, L. V. Goncharova, Q. Zhang, P. Kaghazchi, Q. Sun, A. Lushington, B. Wang, R. Li, X. Sun, *Nano Lett.* **2017**, *17*, 5653.
- [22] a) D. M. Piper, J. J. Travis, M. Young, S. B. Son, S. C. Kim, K. H. Oh, S. M. George, C. Ban, S. H. Lee, *Adv. Mater.* **2014**, *26*, 1596; b) Y. He, D. M. Piper, M. Gu, J. J. Travis, S. M. George, S.-H. Lee, A. Genc, L. Pullan, J. Liu, S. X. Mao, J.-G. Zhang, C. Ban, C. Wang, *ACS Nano* **2014**, *8*, 11816; c) H. Langli Luo, P. Yan, J. J. Travis, Y. Lee, N. Liu, D. Molina Piper, S. Zhang, C. Ban, S.-H. Lee, P. Zhao, S. M. George, J.-G. Zhang, Y. Cui, C.-M. Wang, *ACS Nano* **2015**, *9*, 5559.